Flow Intermittency, Dispersion, and Correlated Continuous Time Random Walks in Porous Media

Pietro de Anna, Tanguy Le Borgne, Marco Dentz, Alexandre M. Tartakovsky, Diogo Bolster, and Philippe Davy

Phys. Rev. Lett. **110**, 184502 — Published 1 May 2013

DOI: 10.1103/PhysRevLett.110.184502

Flow Intermittency, Dispersion and Correlated Continuous Time Random Walks in Porous Media

Pietro de Anna[1,5*] and Tanguy Le Borgne[1], Marco Dentz[2],
Alexandre M. Tartakovsky[3], Diogo Bolster[4], Philippe Davy[1]
[1] *UMR 6118, CNRS, Universite de Rennes 1, France,*
[2] *Spanish National Research Council (IDAEA-CSIC), Spain,*
[3] *Pacific Northwest National Laboratory, WA 99354, USA,*
[4] *University of Notre Dame, IN 46545, USA*
[5] *Massachusetts Institute of Technology, MA 02139, USA*

We study the intermittency of fluid velocities in porous media and its relation to anomalous dispersion. Lagrangian velocities measured at equidistant points along streamlines are shown to form a spatial Markov process. As a consequence of this remarkable property, the dispersion of fluid particles can be described by a continuous time random walk with correlated temporal increments. This new dynamical picture of intermittency provides a direct link between the microscale flow, its intermittent properties, and non-Fickian dispersion.

The heterogeneity of natural flows strongly affects transport, mixing and chemical reactions, including contaminant spreading, effective reaction kinetics and biological activity [e.g. 1–9]. In porous media the complexity of flow arises from the heterogeneous medium structure [10]. This induces non-Gaussian velocity distributions, which can lead to a persistent non-Fickian dispersion regime [3, 11–13]. Various stochastic models have been proposed to represent this property, with very different underlying mechanisms, such as mobile-immobile mass exchange, long-range correlated spatial motions or heavy-tailed trapping time distributions [14–18]. These different models may provide equally good fits to data, such as first passage time distributions [19, 20]. Yet, their implications can be dramatic when transport controlled processes are considered, such as chemical reactions or biofilm growth [7, 19]. A key challenge is to relate these upscaled flow models to the microscale flow properties. In this Letter, we demonstrate the existence of persistent intermittent properties of Lagrangian velocities in porous media and we formulate a new dynamical picture of intermittency based on the spatial Markov property of Lagrangian velocities. The resulting upscaled transport model is a correlated CTRW, which is fully consistent with the microscale flow dynamics.

We consider a two dimensional porous medium composed of circular grains, with a poly-dispersed size distribution and a porosity $\phi = 0.42$ (Fig.1). Flow is described by the Navier-Stokes equation. No-slip conditions are applied at the fluid-solid interface. A constant pressure gradient from left to right induces fluid flow in the pore space. Periodic boundary conditions are applied for the flow velocity at all boundaries. The flow problem is solved using smoothed particle hydrodynamics (SPH). SPH is a Lagrangian particle method that represents elementary fluid volumes as fluid particles which advect with the flow. In the pore-scale flow simulations we used the sixth-order Schoenberg spline function with the support of the weighting function $h = 1$. The size of the domain was 512×128, with 16 particles per pixel, thus, the total number of particles is $N = 1048576$. The number of fluid particles is $N \times \phi = 1048576 \times 0.42 = 440402$. Full details of the method as applied to the current configuration are available in [21]. Streamlines of the flow field are

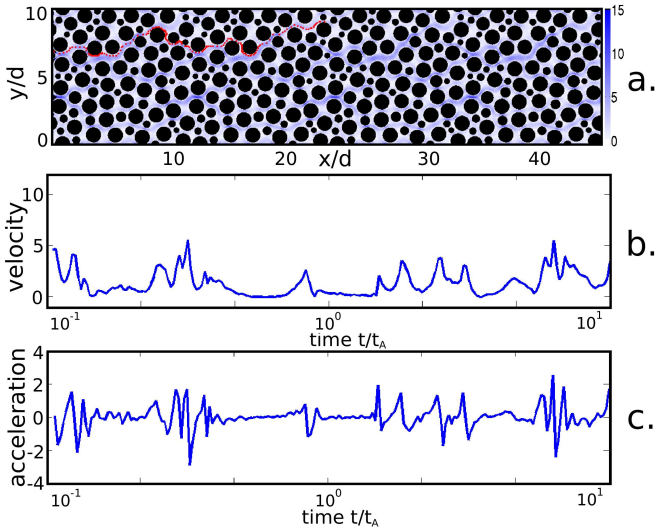

Figure 1. a) The amplitude of the pore scale velocity field normalized by the average Lagrangian velocity. Space is rescaled with respect to the average pore size $d = 10$. The trajectory of a Lagrangian particle is shown with red dots at equidistant time increments $\Delta t = 6 \cdot 10^{-2} t_A$. Time is rescaled with respect to $t_A = d/\overline{v}$, the mean advection time over the mean pore size. b) and c) are respectively the time series of the Lagrangian velocity and acceleration for the particle trajectory displayed on the top.

given by the Lagrangian trajectories $\mathbf{x}(t) = [x(t), y(t)]^T$ of the fluid particles. Figure 1a shows the simulated pore-scale velocity field. It is characterized by high velocity channels and localized low velocity regions.

The spreading of the fluid particles, a measure for purely advective hydrodynamic dispersion, is characterized by the mean-squared longitudinal displacement, $\sigma_x^2(t) = \langle [\Delta x(t) - \langle \Delta x(t) \rangle]^2 \rangle$ with $\Delta x(t) = x(t) - x(0)$. Angular brackets denote the average over all fluid particles. Dispersion of the fluid particles is found to be superdiffusive over two orders of magnitude in time, which means that σ_x^2 evolves faster than linearly [15]; see Fig. 2. Moreover, the higher-order moments of the displacement of fluid particles indicates that the dispersive pro-

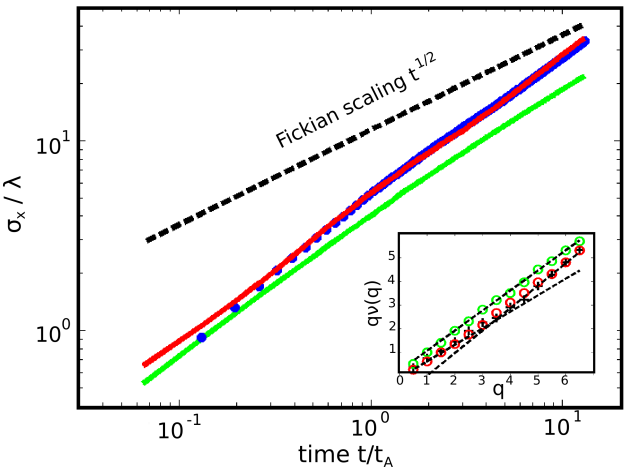

Figure 2. Normalized mean squared longitudinal displacement of purely advected particles versus normalized time. The result of the pore scale simulations is shown as blue dots, the prediction of the correlated CTRW model is shown as a continuous red line, and the prediction of the uncorrelated CTRW model as a continuous green line. The Fickian scaling, shown as a black dashed line, is not reached during the simulation time. λ is the correlation length of the velocity field, see Fig. 5. Inset: black crosses represent the scaling exponents $q\nu(q)$ of the moments of the displacement Δx for the pore scale model; red circles represent the correlated CTRW model, green circles the uncorrelated CTRW model.

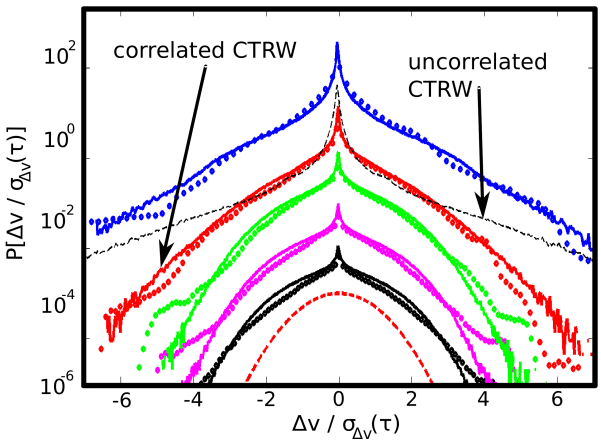

Figure 3. Probability distributions of normalized Lagrangian longitudinal velocity increments $\Delta v/\sigma_{\Delta v}(\tau)$ for the time lags (blue) $\tau = \tau_0$, (red) $2\tau_0$, (green) $5\tau_0$, (magenta) $7\tau_0$, and (black) $9\tau_0$ ($\tau_0 = 6 \times 10^{-2} t_A$). The curves are shifted along the y-axis for clarity. W for each lag time . Dots represent the pore scale SPH simulations data and the solid lines the result of the correlated CTRW model. As the time lag increases the probability distributions approach, without reaching, a Gaussian distribution represented with the red dashed line. The black dashed line represents the result of the corresponding uncorrelated CTRW model for the case $\tau = 2\tau_0$.

cess is strongly anomalous [22] because the scaling exponent $\nu(q)$, defined by

$$\langle |\Delta x(t) - \langle \Delta x(t) \rangle|^q \rangle \sim t^{q\nu(q)},$$

is such that $\nu(2) > 1/2$ and $q\nu(q)$ is not a linear function of q. Notice that this anomalous behavior is expected to persist until the largest velocity correlation time as discussed below.

A sample particle trajectory is displayed in Fig. 1a. The time series of longitudinal Lagrangian velocities $v(t)$ and accelerations $a(t)$ along the trajectory are plotted as a function of travel time in Figures 1b and 1c. The temporal behavior of Lagrangian acceleration is intermittent, switching between low variability periods and strongly fluctuating periods. The first behavior corresponds to low velocity regions, where Lagrangian longitudinal velocities and accelerations are small and strongly correlated. The second behavior corresponds to high velocities in flow channels, where acceleration fluctuations are large. Similar intermittent behaviors have been observed in a series of dynamical systems including turbulent flows [23–26], fluidized beds [27], earthquake occurrences [28], see also the review by Friedrich et al. [7]. While this process has not been documented to date for flow in porous media, we argue that is a key to understanding the persistence of anomalous transport regimes in such systems. To quantify the correlation and statistics of Lagrangian accelerations, we define the Lagrangian velocity increment associated to the time lag τ as

$$\Delta_\tau v = v(t+\tau) - v(t). \qquad (1)$$

The variance of the $\Delta_\tau v$ is denoted in the following by $\sigma^2_{\Delta v}(\tau)$. The probability density function (pdf) of longitudinal Lagrangian velocity increments normalized with respect to the standard deviation of increments, $P[\Delta_\tau v/\sigma_{\Delta v}(\tau)]$ is plotted in Fig. 3 for different time lags τ. For small τ, the distribution of Lagrangian velocity increments is characterized by exponential tails and a sharp peak close to zero acceleration due to the low velocity areas where particles are almost at rest. As τ increases, the slopes of the tails increase and the sharpness of the peak decreases, approaching a Gaussian distribution. The Gaussian shape is however not reached, even for large τ, which is consistent with the fact the Fickian dispersion regime is not attained during the simulation time (Fig. 2). Note also that the sharp peak associated with the zero velocity increment is not observed for turbulent flows [23]. It is associated here with the small velocity variations in the stagnation zones of the porous medium.

The correlation of Lagrangian accelerations $a(t) = dv(t)/dt$ can be quantified by the correlation function,

$$\chi_a(\tau) = \frac{\langle [a(t+\tau) - \langle a \rangle][a(t) - \langle a \rangle] \rangle}{\sigma_a^2}, \qquad (2)$$

where σ_a^2 is the variance of Lagrangian accelerations. Fig. 4 displays the autocorrelation of longitudinal Lagrangian acceleration a and its amplitude $|a|$. The correlation function $\chi_a(\tau)$ decreases rapidly with the time lag τ. The slight anti-correlation at early times is likely due to the rapid fluctuations of acceleration in high velocity channels (Fig. 1c). The correlation of the absolute value of longitudinal Lagrangian acceleration $|a(t)|$ decays slowly

with an approximate power law decay (Fig. 4). Intermittency is often associated with an exponential decay of the acceleration amplitude correlation, which leads to a fast convergence to Gaussianity [23, 24]. The persistent intermittency observed here implies that the multifractal formalisms often used for modeling intermittent properties of time series in dynamical systems may not be relevant for porous media flows. In order to identify

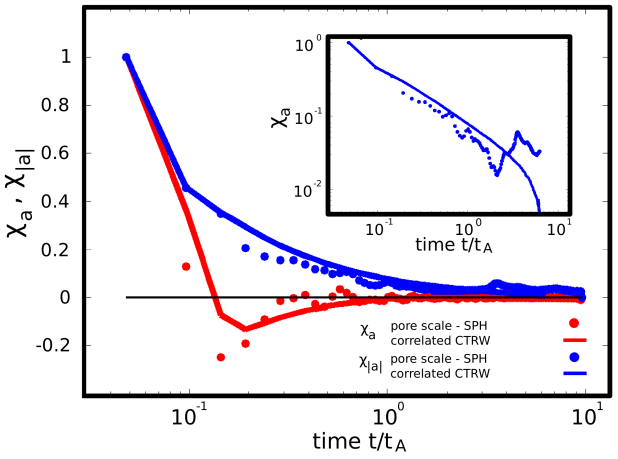

Figure 4. Comparison between pore scale numerical simulations (solid lines) and the correlated CTRW model (dots).The autocorrelation function χ_a of Lagrangian particles accelerations a is represented in red and that of the absolute accelerations $|a|$ is represented in blue. The temporal evolution of the correlation of the absolute acceleration is represented in log-log in inset.

the model that can describe the observed intermittent behavior, we analyze the autocorrelation function of the longitudinal Lagrangian velocity (Fig. 5). Specifically, we consider the autocorrelation of Lagrangian velocities measured at equidistant times along trajectories, as well as measured at equidistant spatial positions. In the first case, the autocorrelation function is given by $\chi_{vt}(\tau) = \langle [v(t+\tau) - \langle v \rangle][v(t) - \langle v \rangle] \rangle / \sigma_{vt}^2$. In the second case, it is given by $\chi_{vx}(\xi) = \langle [v[t(x+\xi)] - \langle v \rangle][v[t(x)] - \langle v \rangle] \rangle / \sigma_{vx}^2$, where $t(x+\Delta x) = t(x) + \Delta x / v[t(x)]$, see, e.g., Ref. [29]. The autocorrelation function $\chi_{vt}(\tau)$ in time is found to decay slowly, and approximately as a power-law with time, $\chi_{vt} \propto (\tau/t_A)^{-0.7}$. The autocorrelation function in space $\chi_{vx}(\xi)$, in contrary, is well represented by an exponential with correlation length $\lambda = d/4$ as illustrated in Fig. 5. The oscillations in the correlation function are due to alternation of pore body and pore throats along particle trajectories over the mean pore size d. The existence of a finite correlation length λ allows for the definition of a characteristic correlation time $\tau_c = \lambda / v_{\min}$ with $v_{\min}$ the minimum fluid particle velocity. Thus, the non Fickian dispersion and flow intermittency regime is expected to persist until τ_c.

The short range spatial correlation of Lagrangian velocities implies a spatial Markov property for velocity transitions over the correlation scale λ. This leads naturally to the following correlated CTRW model for the

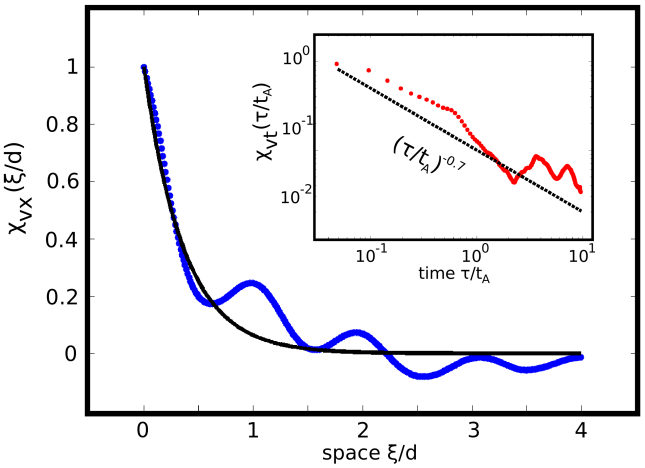

Figure 5. The blue dots represent the Correlation of pore scale Lagrangian velocities in rescaled space $x' = x/d$. The black curve is an exponential fit of the data from which we compute a correlation length of $\lambda = d/4$. In the inset the simulated pore scale Lagrangian velocities correlation in time t/t_A.

motion of fluid particles in x–direction [29, 30]

$$x_{n+1} = x_n + \lambda, \qquad t_{n+1} = t_n + \tau_n,$$

where the transit time τ_n is a Markov process, defined by the pdf $\psi(\tau)$ of transition times and the conditional pdf $\psi(\tau|\tau')$ of successive transit times. Both $\psi(\tau)$ and $\psi(\tau|\tau')$ are determined from the simulated particle trajectories. The transition time is given by $\tau_n = \lambda / v_n$ with v_n the average particle velocity over λ. Hence, the waiting time distribution $\psi(\tau)$ is related to the velocity distribution $p_v(v)$, derived from pore scale simulations, as $\psi(\tau) = p_v(\lambda/\tau)\lambda/\tau^2$. Similarly, the conditional density is given in terms of $p_v(v|v')$ as $\psi(\tau|\tau') = p_v(\lambda/\tau|\lambda/\tau')\lambda/\tau^2$. Note that this formulation is fully determined by the velocity field properties and does not involve any fitting parameter. The particle density is given by $p(x,t) = \langle \delta(x - x_{n_t}) \rangle$, where n_t is the renewal process $n_t = \max(n|t_n \le t)$. The density $p(x,t)$ can be described by the following system of equations

$$p(x,t) = \int_0^t dt' \int_{t-t'}^{\infty} d\tau R(x,t',\tau) \tag{3}$$

$$R(x,t,\tau) = \delta(x - x_0)\psi(\tau)\delta(t) + \int_0^t d\tau' R(x-\lambda, t-\tau', \tau')\psi(\tau|\tau'), \tag{4}$$

with x_0 the initial particle position at time $t = 0$.

The acceleration a_n in step n is related to the spatial and temporal increments λ and τ_n as,

$$\lambda = v_{n-1}\tau_n + \int_{t_n}^{t_n+\tau_n} dt' \int_{t_n}^{t'} dt'' a_n, \tag{5}$$

where v_{n-1} is the velocity at the end of the previous step. Assuming a constant acceleration over each CTRW step and continuity of velocity at turning points, we obtain

$$a_n = \frac{2\lambda}{\tau_n^2} - \frac{2v_{n-1}}{\tau_n}, \qquad v_n = v_{n-1} + a_n\tau_n. \tag{6}$$

The correlated CTRW model correctly predicts both the scaling and the magnitude of the dispersion scale σ_x at all times (Fig. 2). Furthermore, the distribution of velocity increments obtained from the correlated CTRW simulations for different time lags τ are in good agreement with those obtained from the full pore-scale simulations (Fig. 3). The correlated CTRW also predicts correctly the long-range correlation of the acceleration amplitude and the slight anti-correlation of acceleration (Fig. 4). Note that neglecting the correlation of successive transit times in the CTRW model (uncorrelated CTRW) leads to an underestimation of particle dispersion, see Fig 2. It also leads to overestimation of the probability of large velocity increments at small lag times (Fig. 3). The effect of transit time correlation is to reduce the probability of excessively large accelerations, which would be physically inconsistent with flow conservation. Hence, while in many applications the assumption of uncorrelated temporal increments is convenient and allows for simple developments, for transport in divergence-free velocity fields it is not valid. Furthermore, correlations between consecutive velocities, thus, temporal increments, are expected to impact the scaling properties of dispersion in CTRW frameworks [29–35].

The correlated CTRW model provides a new dynamical picture of intermittency and an upscaled transport model, which is fully consistent with the microscale flow dynamics. At the root of this model is the spatial Markov property of Lagrangian velocities, which implies that low particle velocities have a much stronger correlation in time than high velocities. This approach may therefore be an alternative for understanding and quantifying intermittent behaviors in dynamical systems.

Acknowledgements

P. de Anna and T. Le Borgne acknowledge the financial support of the European Commission through FP7 projects ITN project, IMVUL project (Grant Agreement 212298) and Marie Curie ERG grant ReactiveFlows (Grant Agreement Number 230947). A. Tartakovsky was supported by the ASCR Office of the US Department of Energy. D. Bolster was supported by NSF grant EAR-1113704. M. Dentz acknowledges the support of the FP7 EU project PANACEA (Grant Agreement No. 282900).

* E-mail: pietrodeanna@gmail.com - pdeanna@mit.edu

[1] G. Falkowich, K. Gawedzki, and M. Vergassola, Rev. Mod. Phys. **73**, 913 (2001).

[2] J. D. Seymour, J. P. Gage, S. L. Codd, and R. Gerlach, Phys. Rev. Lett. **93**, 198103 (2004).

[3] B. Berkowitz, A. Cortis, M. Dentz, and H. Scher, Rev. of Geophys. **44**, 2 (2006).

[4] A. Tartakovsky, D. Tartakovsky, and P. Meakin, Phys. Rev. Lett. **101**, 4 (2008).

[5] B. Bijeljic, P. Mostaghimi, and M. Blunt, Phys. Rev. Lett. **107**, 204502 (2011).

[6] W. Durham, E. Climent, and R. Stocker, Phys. Rev. Lett. **106**, 238102 (2011).

[7] R. Friedrich, J. Peinke, M. Sahimi, and M. R. R. Tabar, Phys. Rep. **506**, 87162 (2011).

[8] F. Toschi and E. Bodenschatz, Annual Review of Fluid Mechanics **41**, 375 (2009).

[9] G. Boffetta, F. De Lillo, and F. Musacchio, Phys. Rev. E **85**, 066322 (2012).

[10] M. Sahimi, *Flow and Transport in Porous Media and Fractured Rock* (Wiley-VCH, 2011).

[11] D. L. Koch and J. F. Brady, Phys. Fluids A **31**, 965 (1988).

[12] M. Sahimi, Phys. Rev. E **85**, 0162316 (2012).

[13] T. Le Borgne, D. Bolster, M. Dentz, P. de Anna, and A. Tartakovsky, Water Resour. Res. **47**, W12538 (2011).

[14] E. W. Montroll and G. H. Weiss, J. Math. Phys. **6**, 167 (1965).

[15] J. P. Bouchaud and A. Georges, Phys. Rep. **195**, 127 (1990).

[16] J. H. Cushman, X. Hu, and T. R. Ginn, J. Stat. Phys. **75**, 859 (1994).

[17] B. Berkowitz and H. Scher, Phys. Rev. E **57**, 5858 (1998).

[18] M. Meerschaert, D. Benson, and B. Bäumer, Phys. Rev. E **59**, 5026 (1999).

[19] M. Magdziarz, A. Weron, and K. Burnecki, Phys. Rev. Lett. **103**, 180602 (2009).

[20] M. Dentz and D. Bolster, Phys. Rev. Lett. **105**, 244301 (2010).

[21] A. M. Tartakovsky, P. Meakin, T. D. Scheibe, and B. D. Wood, Water Resources Research **43**, W05437 (2007).

[22] P. Castiglione, A. Mazzino, P. Muratore-Gianneschi, and A. Vulpiani, Physica D **134**, 75 (1999).

[23] N. Mordant, J. Delour, E. Léveque, a. Arnéodo, and J.-F. Pinton, Phys. Rev. Lett. **89**, 254502 (2002).

[24] B. Kadoch, W. J. T. Bos, and K. Schneider, Phys. Rev. Lett. **105**, 145001 (2010).

[25] L. Chevillard, S. G. Roux, E. Leveque, N. Mordant, J.-F. Pinton, and A. Arneodo, Phys. Rev. Lett. **91**, 214502 (2003).

[26] a. Arnèodo, R. Benzi, J. Berg, L. Biferale, E. Bodenschatz, a. Busse, E. Calzavarini, B. Castaing, M. Cencini, L. Chevillard, R. Fisher, R. Grauer, H. Homann, D. Lamb, a. Lanotte, E. Lévèque, B. Lüthi, J. Mann, N. Mordant, W.-C. Müller, S. Ott, N. Ouellette, J.-F. Pinton, S. Pope, S. Roux, F. Toschi, H. Xu, and P. Yeung, Phys. Rev. Let. **100**, 254504 (2008).

[27] F. Ghazemi, M. Sahimi, M. Reza Rahimi Tabar, and J. Peinke, J. Stat. Mech. **7**, 07008 (2012).

[28] P. Manshour, S. Saberi, M. Sahimi, J. Peinke, A. F. Pacheco, and M. Reza Rahimi Tabar, Phys. Rev. Lett. **102**, 014101 (2009).

[29] T. Le Borgne, M. Dentz, and J. Carrera, Phys. Rev. Let. **101**, 090601 (2008).

[30] P. Kang, M. Dentz, T. Le Borgne, and R. Juanes, Phys. Rev. Lett. **107**, 180602 (2011).

[31] M. Montero and J. Masoliver, Phys. Rev. E **76**, 61115 (2007).

[32] J. Weiss, Phys. Rev. E **77**, 056106 (2008).

[33] A. V. Chechkin, M. Hofmann, and I. M. Sokolov, Phys. Rev. E **80**, 31112 (2009).

[34] V. Tejedor and R. Metzler, J. Phys. A: Math. Theor. **43**, 82002 (2010).

[35] M. Magdziarz, R. Metzler, R. Szczotka, and P. Zebrowski, J. Stat. Mech. **04**, P04010 (2012).